



UNIVERSITY OF LEEDS

This is a repository copy of *Highly Porous Hydrogen-Bond Networks from a Triptycene-Based Catechol*.

White Rose Research Online URL for this paper:
<http://eprints.whiterose.ac.uk/99858/>

Version: Accepted Version

Article:

Greatorex, S and Halcrow, MA orcid.org/0000-0001-7491-9034 (2016) Highly Porous Hydrogen-Bond Networks from a Triptycene-Based Catechol. *CrystEngComm*, 18 (25). pp. 4695-4698.

<https://doi.org/10.1039/c6ce00966b>

© 2016, The Royal Society of Chemistry. This is an author produced version of a paper accepted for publication in *CrystEngComm*. Uploaded in accordance with the publisher's self-archiving policy.

Reuse

Unless indicated otherwise, fulltext items are protected by copyright with all rights reserved. The copyright exception in section 29 of the Copyright, Designs and Patents Act 1988 allows the making of a single copy solely for the purpose of non-commercial research or private study within the limits of fair dealing. The publisher or other rights-holder may allow further reproduction and re-use of this version - refer to the White Rose Research Online record for this item. Where records identify the publisher as the copyright holder, users can verify any specific terms of use on the publisher's website.

Takedown

If you consider content in White Rose Research Online to be in breach of UK law, please notify us by emailing eprints@whiterose.ac.uk including the URL of the record and the reason for the withdrawal request.



eprints@whiterose.ac.uk
<https://eprints.whiterose.ac.uk/>

Highly Porous Hydrogen-Bond Networks from a Triptycene-Based Catechol

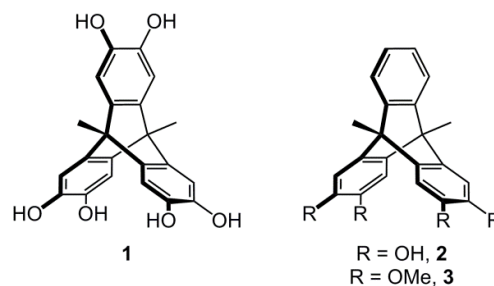
Sam Greatorex and Malcolm A. Halcrow*

Solvate crystals of 9,10-dimethyl-2,3,6,7,14,15-hexa(hydroxy)-triptycene (**1**) form a variety of 3D hydrogen-bonded topologies, including *bcu*, *acs*, *bsn* and an apparently new 7-connected net. Several of these networks contain 1D or 2D arrays of solvent-filled channels, amounting to up to 60 % solvent-accessible void space.

Triptycene derivatives are finding increasing use as scaffolds for supramolecular architectures,¹⁻⁶ in polynucleating ligands for transition ions⁷⁻¹² and for polymeric materials.¹³⁻¹⁵ Diamino-substituted phenylene residues in triptycenes are readily converted by Schiff base condensations into extended arenes,¹⁶ annelated heterocycles^{11,12} or polydentate metal-binding domains.⁸⁻¹⁰ Alternatively, catechol functions in triptycene derivatives have been used as components in hydrogen-bonded supramolecular assemblies, or incorporated into larger crown ether receptors¹⁻⁵ or microporous polymer materials.¹³⁻¹⁵ Many of these studies make use of the rigid three-fold conformation of the triptycene moiety, which pre-disposes them to form cyclic or porous structures in molecular assemblies¹⁻⁶ or extended solids.^{7,8,13,14,16}

Following our interest in redox-active molecular architectures with *bis*- and *tris*-catechol components,^{17,18} we identified 9,10-dimethyl-2,3,6,7,14,15-hexa(hydroxy)triptycene (**1**) and 9,10-dimethyl-2,3,6,7-tetra(hydroxy)triptycene (**2**; Scheme 1)⁶ as potentially useful components in supramolecular assembly structures. We report here that solvate crystals of **1** adopt a number of novel hydrogen bonded network structures with substantial solvent-supported void space[‡]. Crystal structures of solvates of **2**, and of 9,10-dimethyl-2,3,6,7-tetra(methoxy)triptycene (**3**, ESI[†]), are also briefly described.

Recrystallisation of **1** from alcohol solvents using diethyl ether as antisolvent yields crystals of **1**·2Et₂O[‡]. These adopt



Scheme 1 The triptycene derivatives discussed in this work.

the tetragonal space group *I4₁cd*, with half a molecule of **1** per asymmetric unit spanning a crystallographic *C*₂ symmetry axis. Each molecule donates four, and accepts four, O–H...O hydrogen bonds from nearest neighbour molecules of **1** (Fig. 1), as well as hydrogen bonding to two solvent sites. Thus, each molecule of **1** is eight-connected to a distorted cubic array of neighbour molecules, forming a CsCl (*bcu*) topology net that is distorted by the elongated *c* axis of the tetragonal crystal (ESI[†]).^{20,21}

The triptycene molecules in **1**·2Et₂O[‡] form chequerboard layers in the [001] plane, with each molecule oriented at right angles to its four nearest neighbours within the layer. This arrangement affords a 2D network of interconnected channels along the {110} vectors, of approximate dimensions 4.2 x 4.5 Å (Fig. 2). The channels contain the diethyl ether molecules, which are disordered but well defined in the Fourier map (ESI[†]). Taken in isolation, the network of **1** has a void volume of 2568.3 Å³ per unit cell, or 46.6 % of the cell volume.

Three other solvates of **1** were also obtained, from vapour-diffusion crystallisations using the alternative antisolvent pentane. The solvate **1**·3.4thf adopts a trigonal space group *P3c1*, and is topologically very different from **1**·2Et₂O. The [1·3thf] moieties in the asymmetric unit of **1**·3.4thf occupy general crystallographic sites, but show only small deviations from local *C*₃ symmetry down the centre of the triptycene framework. All the molecules of **1** in **1**·3.4thf are co-aligned,

School of Chemistry, University of Leeds, Woodhouse Lane, Leeds, UK LS2 9JT.
Email: m.a.halcrow@leeds.ac.uk

† Electronic Supplementary Information (ESI) available: full experimental details of the crystallographic data collection and refinements; powder diffraction data; and additional crystallographic Figures and Tables showing the hydrogen bonding in the crystals. CCDC 1440046-1440052. See DOI: 10.1039/x0xx00000x

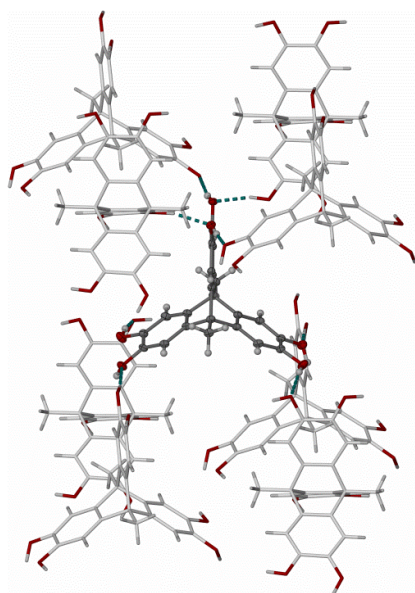


Fig. 1 Packing diagram of **1**·2Et₂O, showing each molecule of **1** hydrogen bonding to an approximately cubic array of eight nearest neighbours. The diethyl ether solvent molecules are not shown, for clarity. Colour code: C, dark grey or white; H, pale grey; O, red.

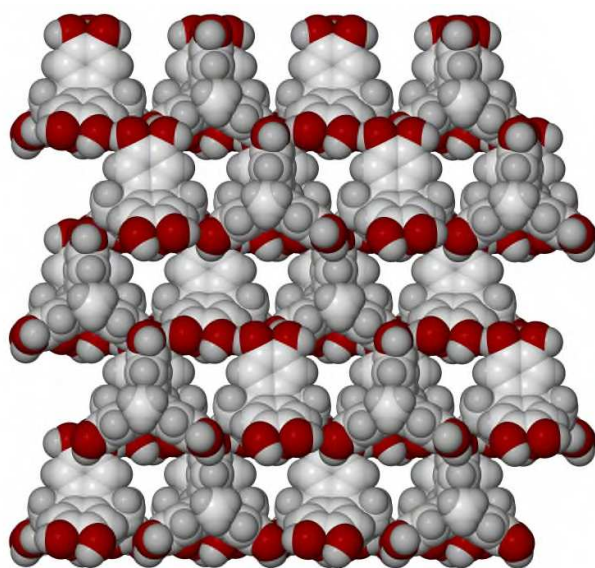


Fig. 2 Space-filling packing diagram of the molecules of **1** in **1**·2Et₂O, showing the channels in the lattice. The view is parallel to the (110) crystal vector, with the *c* axis vertical. An identical series of channels, interconnecting with these ones, occurs at right angles along (110). Colour code: C, white; H, pale grey; O, red.

and hydrogen bond to a trigonal prismatic array of six nearest neighbours in a $4^9.6^6$ (**acs**) net topology (ESI[†]).^{20,21} This leads to *C*₃-symmetric Y-shaped channels parallel to (001), with each arm of the channels being occupied by a resolved, hydrogen-bonded thf molecule (Fig. 3). There is additional void space at the centre of the channels which is occupied by unresolved 0.4-equiv thf according to a *SQUEEZE* analysis.²² Omitting the solvent molecules, the volume of void space in this topology of **1** is 3089 Å³ or 59.6 % of the unit cell, which is substantially higher than for **1**·2Et₂O. The chiral space group adopted by

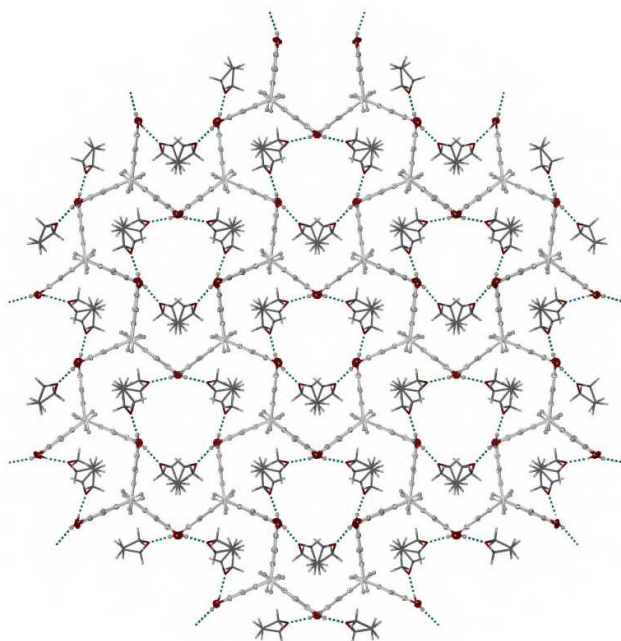


Fig. 3 Packing diagrams of **1**·3.4thf, showing the solvent-filled channels in the lattice. The views are parallel to the (001) crystal vector, with the *a* axis horizontal. Top: view showing the resolved thf sites, with atomic displacement ellipsoids at the 50 % probability level (for **1**) or with arbitrary atomic radii (thf). Bottom: space-filling plot showing the molecules of **1** only. Colour code: C (**1**), white; C (solvent), dark grey; H, pale grey; O, red.

1·3.4thf reflects the asymmetry of the **acs** net, although the absolute chirality of the light atom crystal could not be determined during the structure analysis.

The topology of **1**·2.15CHCl₃ (monoclinic, *C2/c*) is different again, although all the molecules of **1** are also co-aligned along (001). Each molecule of **1** in this lattice is now connected by O–H...O hydrogen bonding to seven nearest neighbours. The resultant hydrogen bond network is an apparently new variant of the class of uninodal 7-connected topologies based on

pillared stacks of 4^4 nets (ESI[†]).²³ In contrast to **1**·3.4thf, whose solvent channels are lined by six-membered molecular circuits of **1** (Fig. 3), **1**·2.15CHCl₃ contains two smaller channel motifs formed from two- and four-membered circuits of **1** (Fig. 4). The smaller channels (*ca.* 4.5 x 6.1 Å) are occupied by disordered, but well defined, molecules of chloroform which do not participate in hydrogen bonding. The contents of the larger channels (5.5 x 14.2 Å) were not resolved, but are probably additional chloroform according to *SQUEEZE*.²² The

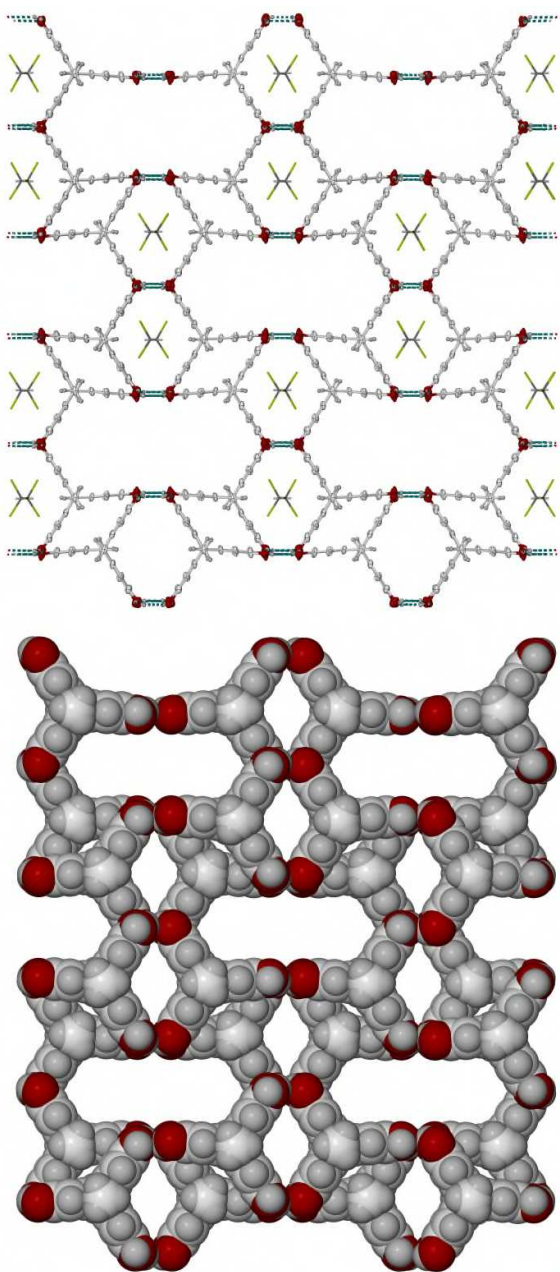


Fig. 4 Packing diagrams of **1**·2.15CHCl₃, showing the solvent-filled channels in the lattice. The views are parallel to the (001) crystal vector, with the *a* axis horizontal. Top: view showing the resolved chloroform sites, with atomic displacement ellipsoids at the 50 % probability level (for **1**) or with arbitrary atomic radii (CHCl₃). Bottom: space-filling plot showing the molecules of **1** only. Colour code: C (**1**), white; C (solvent), dark grey; H, pale grey; O, red.

combined volume of the channels in this network of **1** is 2837 Å³ per unit cell, or 49.8 % of the material.

Unlike the other solvates of **1**, the molecules in **1**·EtOAc (triclinic, $P\bar{1}$) do not form a porous hydrogen-bonded network. Its hydrogen bonding topology is complicated by a disordered hydroxyl group, which donates half-occupied hydrogen bonds to two different acceptors in the lattice. There are three ordered connections between nearest neighbour molecules, which form a 2D puckered 6^3 topology in the $[\bar{1}11]$ plane. The disordered OH group is involved in three additional half-occupied connections, two of them *via* the solvent molecule which accepts two hydrogen bonds from different molecules. If all these connections are considered, the resultant hydrogen bond network corresponds to a $4^8.5^4.6^3$ (**bsn**) 3D net topology, which has racemic helical character (ESI[†]).^{20,21}

Bulk samples of **1**·2Et₂O, **1**·3.4thf and **1**·2.15CHCl₃ are phase-pure and isostructural with the crystalline material by X-ray powder diffraction (ESI[†]). The powder patterns retain their form upon exposure to air at room temperature for 60-80 mins, with slow peak broadening over time indicating gradual loss of crystallinity. However, upon annealing at 370 K for 30 mins all three materials transform to a new phase (**1'**), which was not structurally characterized but is assigned as solvent free **1**. In contrast, microcrystalline samples of **1** crystallized from ethyl acetate/pentane contain predominantly **1'** by powder diffraction, instead of the crystallographic **1**·EtOAc phase. It is unclear whether this reflects the true composition of the sample, or rapid conversion of **1**·EtOAc into **1'** following solvent loss inside the diffractometer.

Two solvates of **2** were also obtained during this study, neither of which is porous. The asymmetric unit of $2 \cdot \frac{1}{2} \text{Et}_2\text{O} \cdot \frac{1}{2} \text{H}_2\text{O} \ddagger$ contains two formula units. It forms a 2D bilayer hydrogen bond network parallel to $[10\bar{2}]$, whose topology depends on the unique water molecule which is disordered between two- and three-connected sites. The crystallographically ordered connections between molecules of **2** afford a binodal five-connected topology, which becomes trinodal if the part-occupied connections to the water are also considered (ESI[†]). In contrast, **2**·dioxane contains just one molecular environment linked to six nearest neighbours, two of them *via* the bridging solvent molecule. The direct contacts between molecules of **2** form a four-connected $6^5.8$ (**dmp**) hydrogen bonded net²¹ which is modified by additional, solvent-bridged diagonal connections between adjacent six-membered rings (ESI[†]). The structure of **3**, an intermediate in the synthesis of **2**, is also shown in the ESI[†].

Conclusions

It has previously been noted that triptycene derivatives are useful scaffolds to support porosity in molecular assemblies or crystalline networks.^{6-8,14-16} These results, in conjunction with another recent study,⁶ highlight that **1** is an attractive and synthetically accessible precursor towards that end. Our current work aims to use **1** as a component in more robust

metal-organic assemblies and frameworks, with potential to combine porosity and redox-active properties.²⁴

Experimental

Compounds **1**, **2** and **3** were prepared by the literature procedures.^{1,4} Other experimental details are in the ESI†.

Acknowledgements

This work was funded by the EPSRC (DTG studentship to SG).

Notes and references

‡ The structures of $1 \cdot 2\text{Et}_2\text{O}$ and $2 \cdot \frac{1}{2}\text{Et}_2\text{O} \cdot \frac{1}{2}\text{H}_2\text{O}$ have been communicated before.¹⁹ However their supramolecular topologies, and the pore structure of $1 \cdot 2\text{Et}_2\text{O}$, were not discussed in this earlier report, and the published structures were not deposited with the CCDC.

- 1 X.-Z. Zhu and C.-F. Chen, *J. Am. Chem. Soc.*, 2005, **127**, 13158.
- 2 X.-Z. Zhu and C.-F. Chen, *Chem. Eur. J.*, 2006, **12**, 5603.
- 3 C. Loholter, M. Brutschy, D. Lubczyk and S. R. Waldvogel, *Beilstein J. Org. Chem.*, 2013, **9**, 2821.
- 4 Q.-S. Zong and C.-F. Chen, *Org. Lett.*, 2006, **8**, 211.
- 5 T. Han and C.-F. Chen, *Org. Lett.*, 2006, **8**, 1069; J.-M. Zhao, Q.-S. Zong and C.-F. Chen, *J. Org. Chem.*, 2010, **75**, 5092; Y. Han, H.-Y. Lu, Q.-S. Zong, J.-B. Guo and C.-F. Chen, *J. Org. Chem.*, 2012, **77**, 2422; Y.-K. Gu, Y. Han and C.-F. Chen, *Supramol. Chem.*, 2015, **27**, 357.
- 6 N. G. White and M. J. MacLachlan, *Chem. Sci.*, 2015, **6**, 6245; N. G. White and M. J. MacLachlan, *Cryst. Growth Des.*, 2015, **15**, 5629.
- 7 J. H. Chong and M. J. MacLachlan, *Inorg. Chem.*, 2006, **45**, 1442.
- 8 J. H. Chong, S. J. Ardakani, K. J. Smith and M. J. MacLachlan, *Chem. Eur. J.*, 2009, **15**, 11824.
- 9 M. Mastalerz, S. Sieste, M. Ceni and I. M. Opperl, *J. Org. Chem.*, 2011, **76**, 6389.
- 10 D. Anselmo, G. Salassa, E. C. Escudero-Adán, E. Martin and A. W. Kleij, *Dalton Trans.*, 2013, **42**, 7962.
- 11 Y. Jiang and C.-F. Chen, *SYNLETT*, 2010, 1679; X. Roy, J. H. Chong, B. O. Patrick and M. J. MacLachlan, *Cryst. Growth Des.*, 2011, **11**, 4551.
- 12 K. A. Williams and C. W. Bielawski, *Chem. Commun.*, 2010, **46**, 5166; S. Gonell, M. Poyatos and E. Peris, *Angew. Chem., Int. Ed.*, 2013, **52**, 7009.
- 13 B. S. Ghanem, M. Hashem, K. D. M. Harris, K. J. Msayib, M. Xu, P. M. Budd, N. Chaukura, D. Book, S. Tedds, A. Walton and N. B. McKeown, *Macromolecules*, 2010, **43**, 5287.
- 14 Y.-C. Zhao, Q.-Y. Cheng, D. Zhou, T. Wang and B.-H. Han, *J. Mater. Chem.*, 2012, **22**, 11509; L. Liu and J. Zhang, *Macromol. Rapid Commun.*, 2013, **34**, 1833.
- 15 T.-Y. Zhou, F. Lin, Z.-T. Li and X. Zhao, *Macromolecules*, 2013, **46**, 7745.
- 16 B. Kohl, F. Rominger, and M. Mastalerz, *Org. Lett.*, 2014, **16**, 704.
- 17 J. J. Loughrey, C. A. Kilner, M. J. Hardie and M. A. Halcrow, *Supramol. Chem.*, 2012, **24**, 2.
- 18 J. J. Loughrey, S. Sproules, E. J. L. McInnes, M. J. Hardie and M. A. Halcrow, *Chem. Eur. J.*, 2014, **20**, 6272; J. J. Loughrey, N. J. Patmore, A. Baldansuren, A. J. Fielding, E. J. L. McInnes, M. J. Hardie, S. Sproules and M. A. Halcrow, *Chem. Sci.*, 2015, **6**, 6935.
- 19 Y. Han, Y. Jiang and C.-F. Chen, *Chin. Chem. Lett.*, 2013, **24**, 475.
- 20 L. Öhrström and K. Larsson, *Molecule-Based Materials – the Structural Network Approach*, Elsevier, Amsterdam, 2005, p. 314.
- 21 M. O’Keeffe, M. A. Peskov, S. J. Ramsden and O. M. Yaghi, *Acc. Chem. Res.*, 2008, **41**, 1782.
- 22 A. L. Spek, *J. Appl. Cryst.*, 2003, **36**, 7.
- 23 D.-L. Long, A. J. Blake, N. R. Champness, C. Wilson and M. Schröder, *Angew. Chem. Int. Ed.*, 2001, **40**, 2443; J. J. Morris, B. C. Noll and K. W. Henderson, *Chem. Commun.*, 2007, 5191.
- 24 L. Sun, M. G. Campbell and M. Dincă, *Angew. Chem., Int. Ed.*, 2016, **55**, 3566.